# FURIN Inhibition Reduces Vascular Remodeling and Atherosclerotic Lesion Progression in Mice

Gopala K. Yakala,* Hector A. Cabrera-Fuentes,* Gustavo E. Crespo-Avilan,† Chutima Rattanasopa,† Alexandrina Burlacu, Benjamin L. George, Kaviya Anand, David Castaño Mayan, Maria Corlianò, Sauri Hernández-Reséndiz, Zihao Wu, Anne M.K. Schwerk, Amberlyn L.J. Tan, Laia Trigueros-Motos, Raphael Chèvre, Tricia Chua, Robert Kleemann, Elisa A. Liehn, Derek J. Hausenloy, Sujoy Ghosh,‡ Roshni R. Singaraja‡

***Objective***—Atherosclerotic coronary artery disease is the leading cause of death worldwide, and current treatment options are insufficient. Using systems-level network cluster analyses on a large coronary artery disease case-control cohort, we previously identified PCSK3 (proprotein convertase subtilisin/kexin family member 3; *FURIN*) as a member of several coronary artery disease–associated pathways. Thus, our objective is to determine the role of FURIN in atherosclerosis.

***Approach and Results***—In vitro, FURIN inhibitor treatment resulted in reduced monocyte migration and reduced macrophage and vascular endothelial cell inflammatory and cytokine gene expression. In vivo, administration of an irreversible inhibitor of FURIN, α-1-PDX (α1-antitrypsin Portland), to hyperlipidemic *Ldlr*$^{-/-}$ mice resulted in lower atherosclerotic lesion area and a specific reduction in severe lesions. Significantly lower lesional macrophage and collagen area, as well as systemic inflammatory markers, were observed. MMP2 (matrix metallopeptidase 2), an effector of endothelial function and atherosclerotic lesion progression, and a FURIN substrate was significantly reduced in the aorta of inhibitor-treated mice. To determine FURIN's role in vascular endothelial function, we administered α-1-PDX to *Apoe*$^{-/-}$ mice harboring a wire injury in the common carotid artery. We observed significantly decreased carotid intimal thickness and lower plaque cellularity, smooth muscle cell, macrophage, and inflammatory marker content, suggesting protection against vascular remodeling. Overexpression of FURIN in this model resulted in a significant 67% increase in intimal plaque thickness, confirming that FURIN levels directly correlate with atherosclerosis.

***Conclusions***—We show that systemic inhibition of FURIN in mice decreases vascular remodeling and atherosclerosis. FURIN-mediated modulation of MMP2 activity may contribute to the atheroprotection observed in these mice.

***Visual Overview***—An online visual overview is available for this article. **(*Arterioscler Thromb Vasc Biol*. 2019;39:387-401. DOI: 10.1161/ATVBAHA.118.311903.)**

**Key Words:** atherosclerosis ■ coronary artery disease ■ Furin ■ macrophages ■ vascular remodeling



Atherosclerotic coronary artery disease (CAD) is the leading cause of death worldwide,[1] and despite improvements in treatment, significant residual disease still remains,[2] prompting the search for new strategies to treat or prevent this illness.

Although the outlines of disease progression are more or less clear, and more recently, several genes have been individually implicated in disease pathology, the information gained has not translated into mechanism-based treatments of CAD. Current treatments are largely restricted to controlling risk

Received on: July 11, 2017; final version accepted on: January 1, 2019.

From the Translational Laboratories in Genetic Medicine, A*STAR Institute, and Yong Loo Lin School of Medicine, National University of Singapore (G.K.Y., C.R., K.A., D.C.M., M.C., Z.W., A.L.J.T., L.T.-M., R.C., T.C., R.R.S.); Cardiovascular and Metabolic Disorders Program, Duke-NUS Medical School, Singapore (H.A.C.-F., G.E.C.-A., C.R., S.H.-R., D.J.H., S.G.); National Heart Research Institute, National Heart Centre Singapore (H.A.C.-F., G.E.C.-A., B.L.G., S.H.-R., E.A.L., D.J.H., S.G.); Institute of Biochemistry, Medical School, Justus-Liebig-University, Giessen, Germany (H.A.C.-F.); Department of Microbiology, Kazan Federal University, Russian Federation (H.A.C.-F.); Tecnologico de Monterrey, Escuela de Ingenieria y Ciencias, Centro de Biotecnologia-FEMSA, Nuevo Leon, México (H.A.C.-F.); Institute of Cellular Biology and Pathology "Nicolae Simionescu", Bucharest, Romania (A.B.); Department of Metabolic Health Research, The Netherlands Organization for Applied Scientific Research (TNO), Leiden (A.M.K.S., R.K.); Department of Vascular Surgery, Leiden University Medical Center, the Netherlands (R.K.); Institute of Molecular Cardiovascular Research, RWTH, Aachen, Germany (E.A.L.); Human Genetic Laboratory, University of Medicine, Craiova, Romania (E.A.L.); Yong Loo Lin School of Medicine, National University Singapore (D.J.H.); The Hatter Cardiovascular Institute, University College London, United Kingdom (D.J.H.); The National Institute of Health Research, University College London Hospitals Biomedical Research Centre, United Kingdom (D.J.H.); Barts Heart Centre, St Bartholomew's Hospital, London, United Kingdom (D.J.H.); and Biomedical, Biotechnology Research Institute, North Carolina Central University, Durham (S.G.).

*These authors contributed equally to this article as co-first authors.

†These authors contributed equally to this article as co-second authors.

‡These authors contributed equally to this article as co-senior authors.

**The online-only Data Supplement is available with this article at https://www.ahajournals.org/doi/suppl/10.1161/ATVBAHA.118.311903.**

Correspondence to Roshni R. Singaraja, PhD, Translational Laboratories in Genetic Medicine, A*STAR Institute, and Yong Loo Lin School of Medicine, National University of Singapore, 8A Biomedical Grove, Singapore 138648, email rsingaraja@tlgm.a-star.edu.sg; or Sujoy Ghosh, PhD, Cardiovascular and Metabolic Disorders Program, Duke-NUS Medical School, 8 College Rd, Singapore 169857, email sujoy.ghosh@duke-nus.edu.sg

**Nonstandard Abbreviations and Acronyms**

| | |
|---|---|
| **CAD** | coronary artery disease |
| **HDLc** | high-density lipoprotein cholesterol |
| **ICAM** | intercellular adhesion molecule 1 |
| **IL1-β** | interleukin 1β |
| **LDLc** | low-density lipoprotein cholesterol |
| **Ldlr** | low-density lipoprotein receptor |
| **MMP2** | matrix metallopeptidase 2 |
| **PCKS** | proprotein convertase subtilisin/kexin |
| **PDGF** | platelet-derived growth factor |
| **TGF** | transforming growth factor |
| **TNF** | tumor necrosis factor |
| **WTD** | Western-type diet |

factors, such as hypercholesterolemia and hypertension, but do not directly target mechanisms that drive atherosclerotic processes. The lack of mechanism-based interventions is 1 reason why the global burden of atherosclerotic cardiovascular disease continues to rise.

As a first step towards mechanism-based interventions, new approaches to identify putative candidates for therapeutic development are necessary. To this end, we previously conducted a systems analysis of genetic association data from CAD cases and controls (CARDIOGRAM consortium [Coronary Artery Disease Genome-Wide Replication and Meta Analysis][3]). Through pathway enrichment analyses, we identified disease-associated pathways that were enriched for CAD-associated polymorphisms in their component genes.[4] One key finding was the identification of a proprotein convertase of the PCSK (proprotein convertase subtilisin/kexin) family, *FURIN*, as a hub gene shared across 6 of 32 replicated CAD-associated pathways,[4] making FURIN an attractive target for further validation in atherosclerosis.

*FURIN* (*PCSK3*) is a member of the proprotein convertase family that cleave multiple secretory protein precursors at specific single or paired basic amino acids. *Furin* knockout mice die at embryonic day 11 because of cardiac ventral closure defects and hemodynamic insufficiency.[5] However, *Furin*$^{+/-}$ mice are viable, and appear relatively normal, suggesting that ≈50% of FURIN is sufficient to perform most of its critical functions.

FURIN has been implicated in several diseases. In cancer, treatment with FURIN inhibitors reduced various tumors and metastases.[6,7] FURIN expression is increased in the cartilage of patients with osteoarthritis, and treatment of mouse models of arthritis with FURIN inhibitors decreased inflammation and arthritis[8,9]. FURIN inhibition also reduced viral infections in in vitro models.[10,11]

FURIN expression is increased in several cell types in human atherosclerotic lesions.[12] In addition, FURIN expression increased with increasing lesion severity in humans.[13] Liver-specific inhibition of FURIN in mice led to a decrease in atherosclerotic lesions,[14] and FURIN levels were correlated with cardiovascular complications in type 2 diabetics.[15] As well, a large-scale association analysis identified a single nucleotide polymorphism, rs17514846, in *FURIN*, as a risk factor for CAD.[16] Together, these findings suggest a role for FURIN in atherosclerotic cardiovascular disease.

A direct investigation of FURIN function using knockout mice models is difficult because mice with targeted deletions in *Furin* die in utero.[5] However, chemical and peptide-based FURIN inhibitors have been developed and extensively tested in viral and bacterial infections[17] and various types of cancers.[6,18] These inhibitors show significant efficacy in inhibiting FURIN in multiple systems and are commonly used as tool compounds to probe the function of FURIN in cellular and animal models.[19–22] In this study, we utilize inhibition as well as overexpression of FURIN in vivo and show that systemic FURIN levels are directly associated with atherosclerotic lesion progression in mouse models of atherosclerotic cardiovascular disease.

## Materials and Methods

The data that support the findings of this study are available from the corresponding author on reasonable request. Please see the Major Resources Table in the online-only Data Supplement.

### Pathway Enrichment and Gene Expression Omnibus Analyses

To identify novel associations between established biological mechanisms and CAD, we performed a 2-stage pathway-based gene set enrichment analysis of 16 genome-wide association study datasets for CAD (available through the CARDIOGRAM consortium). Pathway enrichment analysis was conducted via the i-GSEA4GWAS (http://gsea4gwas.psych.ac.cn/inputPage.jsp) tool[23] by querying the Reactome pathway database.[24] From a meta-analyzed discovery cohort of 7 CAD genome-wide association study datasets (9889 cases/11 089 controls), nominally significant pathways were tested for replication in a meta-analysis of 9 additional studies (15 502 cases/55 730 controls).

To examine *FURIN* gene expression levels in atherosclerosis-relevant samples from human sources, we screened the Gene Expression Omnibus for human studies identified by the keywords macrophages, vascular endothelial cells, vascular smooth muscle cells, and atherosclerotic plaques. 18 microarray studies (Affymetrix and Illumina platforms), encompassing 570 samples were ultimately retrieved and analyzed. We queried the expression of *FURIN* and other proprotein convertases in samples from the different biological sources. To enable comparisons between diverse Gene Expression Omnibus datasets, the expression values from each study were converted into quintiles with Q1 representing the upper 20% and Q5 the bottom 20% of all expression values.

### Western-Type Diet Fed *Ldlr*$^{-/-}$ Model of Atherosclerosis

All experiments were approved by the Biomedical Sciences Institute Singapore Institutional Animal Care Committee and adhered to the Recommendation on Design, Execution, and Reporting of Animal Atherosclerosis Studies by the American Heart Association.[25] Thirty-two male *Ldlr*$^{-/-}$ mice (C57BL/6JInv, Jackson Laboratory) on a 12-hour light-dark cycle were maintained on chow diet (1324_modified, Altromin GmbH & Co) until 12 weeks of age, followed by a Western-type diet (WTD; D12079B, Research Diets, NJ) for 8 weeks. Half the mice were injected intraperitoneally with 1x PBS and the other half with 100 μg/kg of FURIN inhibitor (α-1-PDX [α1-antitrypsin Portland], RP-070; Thermo Fisher Scientific), twice per week, for 8 weeks in conjunction with the WTD feeding. The mice had free access to food and water except during a 4 to 5 hours fast period before blood sample collection. Mice were anesthetized at 20 weeks (100 mg/kg ketamine hydrochloride/10 mg/kg xylazine IP), bled retroorbitally, perfused transcardially with 1x PBS, and hearts fixed in 4% paraformaldehyde (Sigma) and embedded in paraffin. Livers, aortic arch, and thoracic aorta were snap-frozen in liquid $N_2$ and stored at −80°C.

## Plasma FURIN, Inflammatory Markers, and Lipid Quantification

Plasma HDLc (high-density lipoprotein cholesterol), LDLc (low-density lipoprotein cholesterol), and triglycerides were measured by COBAS analyzer (c111, Roche), using kits 05401488, 05401682, and 04657594 (Roche Diagnostics, Switzerland), respectively. Plasma FURIN (E9700m; Wuhan EIAab Science, China), IL1-β (interleukin 1β), TNF (tumor necrosis factor)-α, and TGF (transforming growth factor)-β (R&D Systems) were determined by ELISA following manufacturer's instructions.

## Atherosclerotic Lesion Analyses

Serial cross-sections (5-μm thick) were taken throughout the entire aortic root for histological analyses as described.[26,27] Briefly, aortic cross-sections were stained with hematoxylin-phloxine-saffron and atherosclerotic lesion area was analyzed in 4 cross-sections/mouse. Aperio Imagescope (Leica Biosystems) and ImageJ were used for morphometric quantification of lesion number, area, and severity according to the American Heart Association[26,27] classification. MAC-3 (CD107b; 550292; BD-Pharmigen) and α-SMA (61001; Progen, Germany) antibodies were used to determine macrophage and smooth muscle actin content. Sections were stained with Picrosirius red (365548; Sigma) for collagen content.

## Matrix Metallopeptidase Activity Assays

The aortic arch was dissected, snap-frozen, and homogenized in RIPA (radioimmunoprecipitation assay) buffer. Twenty micrograms protein was mixed with SDS-Tris-glycine sample buffer without a reducing agent, loaded onto a precast 10% SDS–polyacrylamide gel containing 1 mg/mL gelatin (EC6175BOX; Thermo Fisher Scientific), and samples electrophoresed according to manufacturer's protocol (Thermo Fisher Scientific). Mouse recombinant MMP2 (matrix metallopeptidase 2; 554402; Biolegend) and MMP9 (755202; Biolegend) were used as positive controls. Digested bands were quantified by ImageJ software.

## Carotid Artery Wire Injury Model of Vascular Remodeling

Male, 10 to 12-week-old *Apoe*$^{-/-}$ mice (C57BL/6J background) from Charles River Laboratory (Italy) maintained on 12-hour dark/light cycle and fed an atherogenic high-fat diet (21% fat, 0.15% cholesterol; Altromin) for 1 week before and 2 weeks after injury were anaesthetized (100 mg/kg ketamine hydrochloride/10 mg/kg xylazine IP) and subjected to endothelial denudation of the left common carotid artery by a 1 cm insertion of a flexible 0.36-mm guidewire through a transverse arteriotomy of the external carotid artery, as described.[28] For the inhibitor studies, *Apoe*$^{-/-}$ mice were continuously treated with FURIN inhibitor α-1-PDX (20 μg/kg per day) via Alzet osmotic minipumps, subcutaneously implanted 1 day before injury. For the recombinant FURIN expression studies, 2 units of purified human recombinant FURIN (P8077; New England Biolabs, MA) in 20 nmol/L HEPES per mouse was injected 3× per week, intraperitoneally, beginning on the day of wire injury. At 2 weeks after injury, the mice were euthanized and perfused in situ with 4% paraformaldehyde. The injured carotid arteries were isolated, fixed in 4% paraformaldehyde, dehydrated, and embedded in paraffin. Serial 4-μm transverse sections (9 sections/mouse, 40 μm apart) were collected within a distance of 0 to 320 μm from the bifurcation, stained using Elastica-van Gieson, and areas of lumen, neointima (between lumen and internal elastic lamina), and media (between internal and external elastic laminae) were measured by planimetry using Diskus Software (Hilgers). For each mouse, data from the 9 sections were averaged to represent lesion formation along this standardized distance. Neointimal macrophages, smooth muscle cells, and endothelial cells were visualized by immunofluorescence staining for MAC-2 (Galectin-3; M3/38; Cedarlane), SMA (smooth muscle actin; 1A4; Dako), or CD31 (cluster of differentiation 31; M-20; Santa Cruz Biotechnology), respectively, followed by fluorescein isothiocyanate (FITC)–conjugated or Cy3-conjugated secondary antibody staining (Jackson ImmunoResearch) as described.[29,30] Animal studies were approved by local authorities and complied with German animal protection law and also approved by the Biomedical Sciences Institute Singapore Institutional Animal Care Committee.

## Cell Culture and Differentiation

THP-1 (Tohoku Hospital Pediatrics-1) cells were differentiated using 10 ng/mL phorbol 12-myristate-13-acetate (Sigma-Aldrich) for 48 hours, then in RPMI1640 (10% FCS, 1% L-glutamine) for 24 hours. For experiments with THP-1-activated monocytes, cells were stimulated with 100 ng/mL of lipopolysaccharide (LPS-EB Ultrapure; InvivoGen) for 4 hours. FURIN activity assays were performed in THP-1 monocytes and phorbol 12-myristate-13-acetate–differentiated macrophages after 24-hour incubation in the absence or presence of lipopolysaccharide (100 ng/mL) following manufacturer's instructions (New England Biolabs).

Primary human coronary artery endothelial cell line from ATCC (Manassas, VA) was cultured in EndoGRO-VEGF Complete Culture Media (Merck, Kenilworth, NJ) supplemented with 20% FBS, heparin, endothelial cell growth factor, nonessential amino acids, and antibiotics. Human coronary artery endothelial cell line cells (100 000) were placed in 12 well plates and treated with 25 μM Decanoyl-RVKR-CMK (dec-CMK; Merck), recombinant human TNF-α (20 ng/mL, BioLegend), or dec-CMK followed by TNF-α.

## Real-Time Reverse Transcription-Polymerase Chain Reaction

Total RNA was prepared using NucleoSpin RNA Mini kit (Macherey-Nagel), and cDNA was synthesized using iScript cDNA Synthesis Kit (Bio-RAD). Real-time polymerase chain reaction (PCR) analyses were performed on an Applied Biosystems Viia 7 instrument, with PrecisionFASTTM 2X quantitative PCR Mastermix (PrimerDesign). PCR runs included a 2-minute preincubation at 95°C, followed by 50 cycles consisting of 95°C for 5 s, 64°C for 5 s, and 72°C for 10 s. After completion of PCR, a melting curve and Cq value were analyzed. Primer sequences are available on request.

## Statistical Analyses

Data were analyzed using GraphPad Prism (Prism version 7, GraphPad Software). D'Agostino's $K^2$ and Shapiro-Wilk tests were applied to determine the normality of the data. If the data passed the normality tests, differences between 2 groups were analyzed using Student *t* test. If data did not pass normality, Mann-Whitney tests were applied to check for significant differences. One-way ANOVA was used to determine the significant differences for multiple group comparisons, followed by a Tukey post hoc test. For nonparametric multiple comparisons, Kruskal-Wallis tests were used. Dose-response curves of FURIN activity in cultured cells were generated via the DRC software in R, based on a 4-parameter log-logistic model.[31] Values of $P<0.05$ were considered to represent significant differences between groups. Results are shown as mean±SEM.

# Results

## Genetic and Genomic Evidence Support a Role for *FURIN* in Atherosclerosis

Pathway enrichment analyses of genome-wide association studies had previously identified 32 Reactome pathways as replicably associated with CAD.[4] Analyses of pathway interrelationships via sharing of gene components identified FURIN as a central component of 6 CAD-associated Reactome pathways,[32] including degradation of the extracellular matrix, extracellular matrix organization, posttranslational modification (gamma carboxylation, hypusine formation, and arylsulfatase activation), signaling by PDGF (platelet-derived growth factor), signaling by NOTCH, and signaling by TGF-β receptor

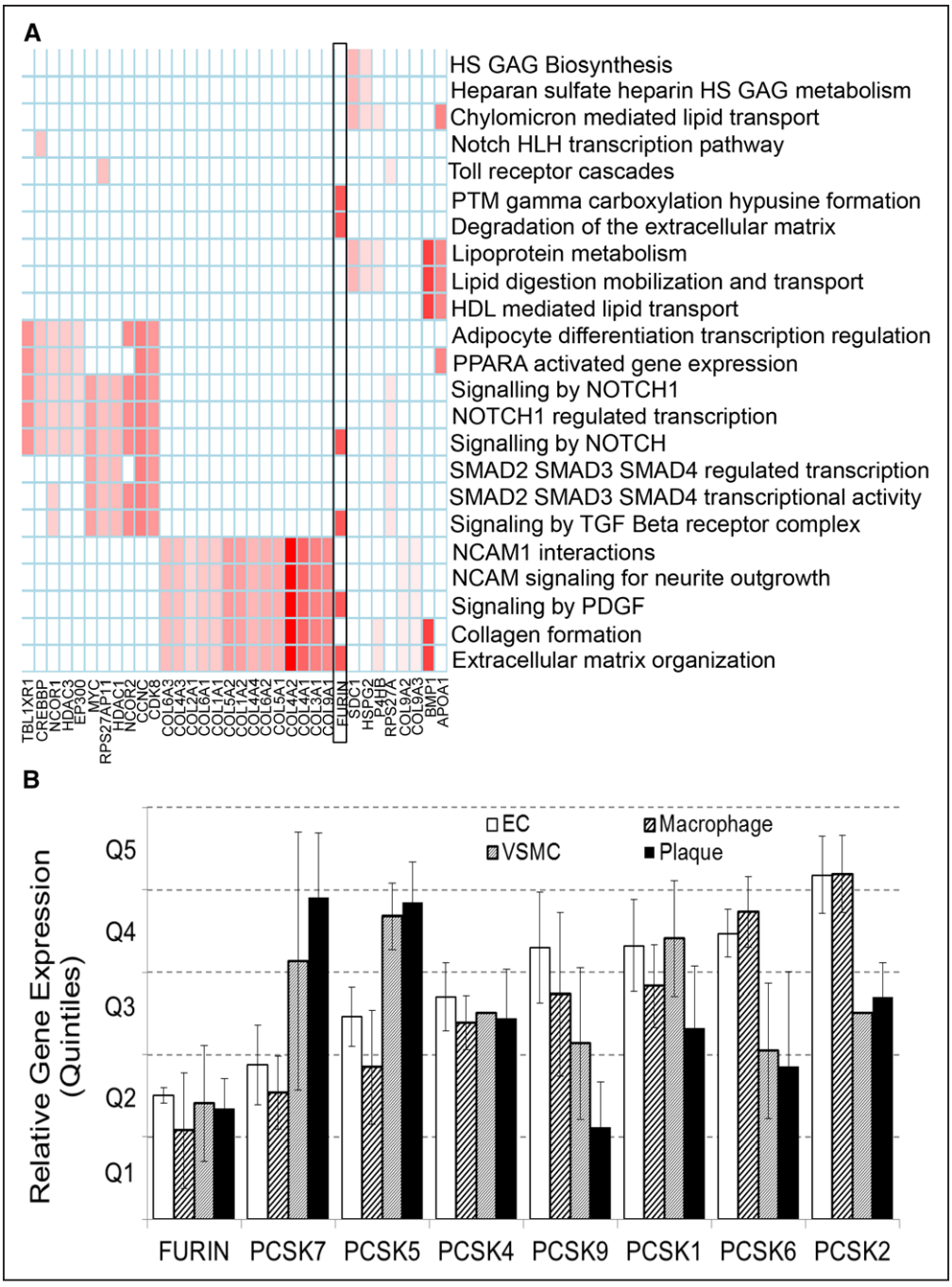


**Figure 1.** Genetic and genomic evidence for the association of *FURIN* with coronary artery disease (CAD). **A**, Heatmap representing genes that are common members of biological pathways significantly associated with CAD.[4] The results for FURIN are highlighted in the black-bordered rectangle. Heatmap is color-coded by the negative logarithm of the CAD-association *P* values for the respective genes. **B**, Expression of FURIN in genome-scale expression datasets in Gene Expression Omnibus. Expression of FURIN and other PCSKs (proprotein convertase subtilisin/kexin family members) were quantified in 570 samples encompassing vascular endothelial cells (EC), vascular smooth muscle cells (VSMC), monocyte/macrophages (Macrophage), and human atherosclerotic plaques (Plaque). To allow comparisons between disparate experiments, gene expression levels were converted to quantiles (quintiles) with quintile 1 (Q1) representing the top 20% expressed genes. HDL indicates high-density lipoprotein; HLH, hemophagocytic lymphohistiocytosis; HS, heparan sulfate; NCAM, neural cell adhesion molecule; PDGF, platelet-derived growth factor; PPARA, peroxisome proliferator-activated receptor alpha; PTM, post-translational modification; SMAD, mothers against decapentaplegic homolog; and TGF, transforming growth factor.

complex (Figure 1A). These findings suggest a possible role for FURIN in vascular remodeling (via extracellular matrix modulation[33] and PDGF signaling pathways[34]), inflammation and cellular infiltration (via Notch and PDGF signaling[34,35]), and regulation of plaque stability (via TGF-β signaling[36]), thereby affecting both early- and late-stage atherosclerotic processes. To evaluate additional evidence for FURIN's potential involvement in atherosclerosis, we screened large-scale gene expression data from the Gene Expression Omnibus[37] for human studies relevant to atherosclerosis, from which 18 microarray studies encompassing 570 samples were retrieved and analyzed. *FURIN* was highly expressed in all

atherosclerosis-relevant cell types (Figure 1B) and in atherosclerotic plaques. Of all proprotein convertases tested, *FURIN* expression was most consistently high in all atherosclerosis-relevant cell types, including plaques. This finding is also consistent with other published data showing high *FURIN* levels in atherosclerotic plaques.[38]

### FURIN Inhibition Decreases Monocyte Migration and Monocyte/Macrophage and Vascular Endothelial Inflammatory Gene Expression In Vitro

Because our Reactome pathway analyses suggested a potential role for FURIN in inflammation and cellular infiltration, we first assessed if FURIN plays a role in monocyte migration. Dose-response curves for FURIN inhibition in monocytes, macrophages, and human coronary artery endothelial cells were determined by treating cells with varying concentrations of the irreversible, cell-permeable, and competitive FURIN inhibitor Decanoyl-RVKR-CMK[39] (Figure I in the online-only Data Supplement). In transwell migration assays, the migration of lipopolysaccharide activated monocytes was significantly decreased in the presence of Decanoyl-RVKR-CMK (Figure 2A), demonstrating that FURIN facilitates the transmigration of monocytes. The decreased number of transmigrated monocytes was not a result of increased cell death in the inhibitor-treated group (Figure 2B). To determine the impact of FURIN inhibition on inflammatory and adhesion molecule expression, we assessed gene expression levels. In monocytes, the expression of the adhesion molecule *VCAM-1* (vascular cell adhesion molecule 1) was significantly reduced in the presence of the inhibitor (Figure 2C). No changes were observed in the expression of the inflammatory markers *CCL2* (C-C motif chemokine ligand 2), *NF-κB* (nuclear factor kappa B subunit 1), and *IL1-β*, as well as the adhesion molecule, *ICAM-1* (intercellular adhesion molecule 1; Figure 2C). Under lipopolysaccharide-stimulated inflammatory conditions in monocytes, a significant inhibition of *ICAM-1* and *IL1-β* expression was observed (Figure 2D), suggesting that FURIN inhibition may reduce monocyte inflammatory cytokine and adhesion molecule expression during atherogenesis. In macrophages, the expression of *CCL2*, *VCAM-1*, and *ICAM-1* were all reduced in the presence of the FURIN inhibitor (Figure 2E), suggesting that inflammatory chemokine, cytokine, and adhesion molecule expression may also be significantly decreased by FURIN inhibition in lesional macrophages. We next assessed the response of FURIN to lipopolysaccharide elicited inflammation and found a significant decrease in macrophage FURIN activity (Figure 2F). This decrease in FURIN activity was not observed in monocytes on lipopolysaccharide stimulation (Figure 2F). Together, these data show that FURIN modulates monocyte recruitment and transmigration and regulates monocyte and macrophage response to inflammatory stimulation.

We next assessed the impact of FURIN inhibition on TNF-α stimulated vascular endothelial cells because FURIN is expressed in and plays a critical role in endothelial cell function.[40] A significant reduction in *NF-κB*, *CCL2*, *IL1-β*, and *VCAM-1* expression was observed (Figure II in the online-only Data Supplement), whereas no changes in *ICAM-1* expression were observed. These data suggest that FURIN inhibition may protect against inflammatory stimulation in both monocyte/macrophages and vascular endothelial cells during atherosclerosis.

### Lower Plasma FURIN Levels in FURIN Inhibitor–Treated Mice

Because our in silico analyses showed *FURIN* to be a hub gene in CAD-associated pathways, its levels were elevated in atherosclerotic plaques, and our in vitro studies suggested FURIN inhibition may be atheroprotective, we next assessed if FURIN plays a role in atherosclerotic lesion development in vivo. We utilized α-1-PDX, a peptide inhibitor of FURIN that functions as a suicide substrate that irreversibly binds to and causes the degradation of the FURIN protein.[21,41] Male, 12-week-old *Ldlr*$^{-/-}$ mice on a WTD were injected thrice per week intraperitoneally with the FURIN inhibitor for 8 weeks. To determine if FURIN inhibitor treatment has an effect on FURIN protein levels in vivo, we quantified plasma levels of FURIN in inhibitor-treated and vehicle-treated control mice. Compared with controls, circulating plasma levels of FURIN were significantly lower (59% decrease, $P$=0.002) in the FURIN inhibitor–treated mice, suggesting that indeed, administration of the FURIN inhibitor α-1-PDX resulted in reduced circulating FURIN levels (Figure IIIA in the online-only Data Supplement).

### Lower Atherosclerotic Lesion Area and Severity in FURIN Inhibitor–Treated *Ldlr*$^{-/-}$ Mice

To determine the impact of FURIN inhibition on atherosclerotic lesion development, the WTD fed *Ldlr*$^{-/-}$ mouse model was utilized.[42] Atherosclerotic lesions were analyzed after 8 weeks of concurrent WTD and α-1-PDX administration in hematoxylin-phloxine-saffron stained sections of the aortic sinus. A trend toward lower total lesion area in the FURIN inhibitor–treated group was observed (FURIN inhibitor: 39.87±5.51; Control: 50.07±6.40×10$^3$ μm$^2$, n=15 each; $P$=0.2; Figure 3A and 3B). Lesions were then categorized using the American Heart Association classification system as mild (class I to III) or severe (classes IV and V).[26,27] No change in the area of mild lesions was observed (FURIN inhibitor: 43.22±9.99; Control: 38.19±8.43×10$^3$ μm$^2$, n=15 each; $P$=0.7; Figure 3C and 3D). However, significantly lower (by 66%) advanced lesion area was observed in the FURIN inhibitor–treated group (FURIN inhibitor: 14.43±6.26; Control: 42.03±11.87×10$^3$ μm$^2$, n=15 each, $P$=0.04; Figure 3D) suggesting that in the *Ldlr*$^{-/-}$ hypercholesterolemic model, FURIN inhibition reduced the formation of more mature lesions.

### FURIN Inhibition Reduces Atherosclerotic Lesion Complexity

Because an overall trend to lower lesion area, and a significant decrease in advanced lesion area, was observed in FURIN inhibitor–treated mice, we next assessed lesion complexity. Significantly lower (by 34%) macrophage (MAC-3)-positive lesion area was observed in the FURIN inhibitor–treated mice (FURIN inhibitor: 102.69±16.45, n=14; Control: 155.09±12.50×10$^3$ μm$^2$, n=15; $P$=0.04; Figure 3E and 3F). The smooth muscle cell area of lesions, assessed by α-smooth

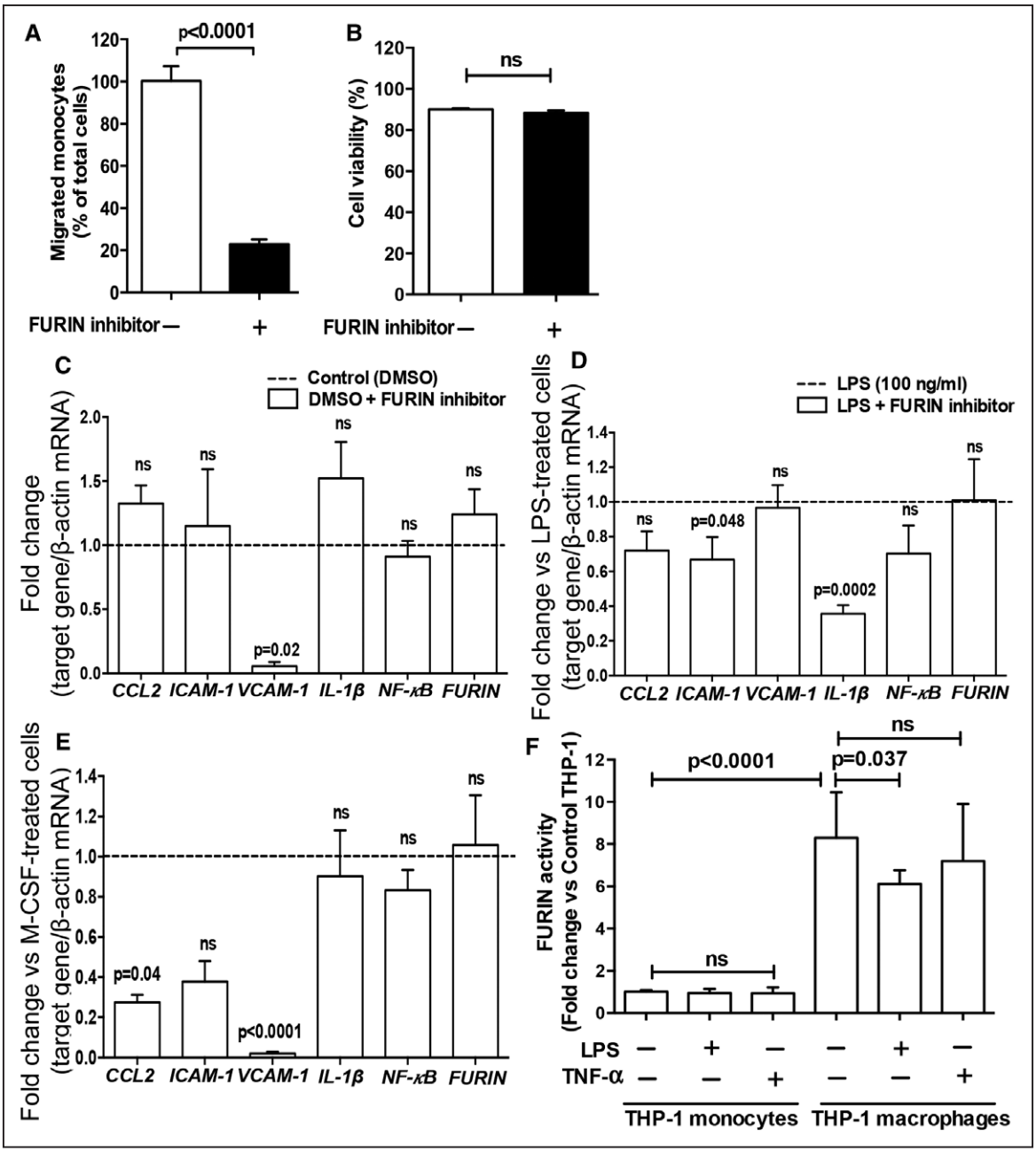


**Figure 2.** FURIN inhibition decreases monocyte migration and inflammatory gene expression in vitro. **A**, Activated human THP-1 (Tohoku Hospital Pediatrics-1) monocytes were subjected to transwell migration assays. In the presence of the FURIN inhibitor Dec-RVKR-CMK, a significantly lower number of monocytes migrated to the chemoattractant M-CSF (macrophage colony-stimulating factor) and (**B**) the lower number of transmigrated monocytes did not result from increased cell death. **C**, Lower *VCAM-1* expression level in FURIN inhibitor–treated monocytes. **D**, *ICAM-1* and *IL1-β* transcription is significantly reduced in FURIN inhibitor–treated monocytes on lipopolysaccharide (LPS) stimulation. **E**, *CCL2* and *VCAM-1* transcription is significantly reduced in FURIN inhibitor–treated M-CSF–derived macrophages. **F**, FURIN activity is significantly decreased in LPS-treated macrophages. Data represent mean±SEM of 3 independent experiments performed in triplicate. The dotted lines in **C**, **D**, and **E** represent control values. Data in **A**, **B**, and **F** were assessed using Student *t* tests. Data in **C**–**E** used Kruskal-Wallis ANOVA tests. DMSO indicates dimethyl sulfoxide; ns, not significant; and TNF, tumor necrosis factor.

muscle actin immunostaining did not significantly differ between the groups (FURIN inhibitor: 46.43±7.72, n=13; Control: 54.36±5.79×10$^3$ μm$^2$, n=14; *P*=0.4; Figure IIIB and IIIC in the online-only Data Supplement), suggesting that FURIN inhibition, in this model, did not decrease plaque cellularity. In addition, Picrosirius red staining showed a significantly lower area of thick mature collagen fibers in lesions (FURIN inhibitor: 72.34±7.91; Control: 109.19±13.59×10$^3$ μm$^2$, n=15 each; *P*=0.02; Figures 3G and 3H), suggesting reduced lesional collagen in FURIN inhibitor–treated mice.

## FURIN Inhibition Reduces Systemic Inflammation in Mice

Because treatment of the WTD fed *Ldlr*$^{-/-}$ mice with α-1-PDX resulted in reduced advanced lesion size and complexity, we next assessed levels of circulatory markers of inflammation in

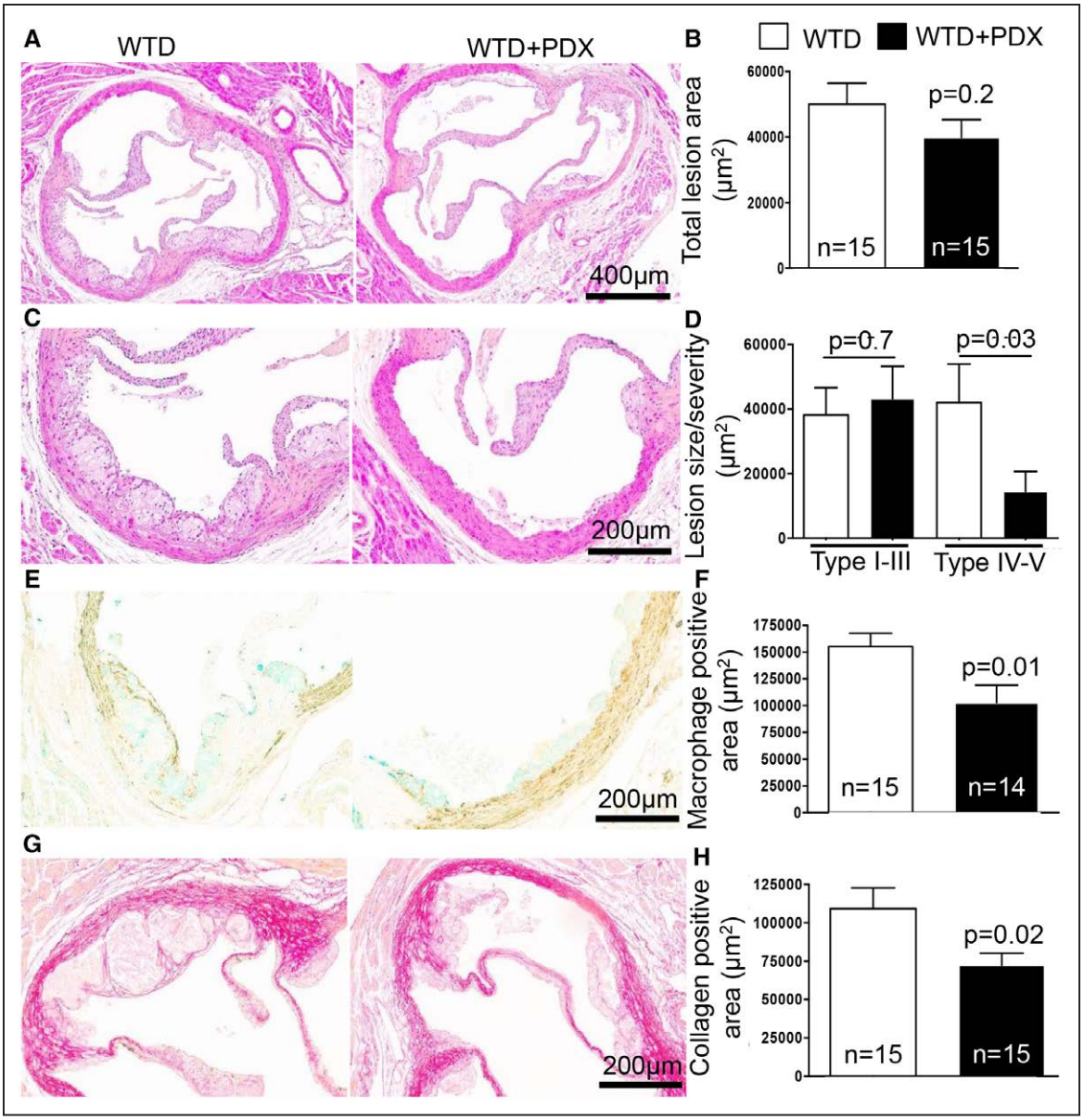


**Figure 3.** Lower lesion complexity and severe atherosclerotic lesion size in FURIN inhibitor–treated mice. **A**, Representative photomicrographs of aortic sinus after histological staining with hematoxylin-phloxine-saffron (×200). **B**, A trend toward lower aortic sinus lesion area in FURIN inhibitor–treated mice. **C**, Representative photomicrographs of lesion severity in aortic sinus after histological staining with hematoxylin-phloxine-saffron (×100). **D**, Significantly lower severe lesion area (type IV and V) in FURIN inhibitor–treated mice. **E**, Representative photomicrographs of macrophages (green) in aortic sinus (×100). **F**, Significantly lower lesional macrophage area in FURIN inhibitor–treated mice. **G**, Representative photomicrographs of aortic root after histological staining with picrosirius red for collagen (×100). **H**, Significantly lower collagen area in lesions of FURIN inhibitor–treated mice. Groups are abbreviated as *Ldlr*$^{-/-}$ mice fed Western-type diet injected with PBS (WTD); *Ldlr*$^{-/-}$ mice fed WTD injected with the α-1-PDX (α1-antitrypsin Portland) FURIN inhibitor (WTD+PDX). All mice are male. Values represent mean±SEM. Data in **F** and **H** are normally distributed, and *P* values were assessed using Student *t* tests. Data in **B** and **D** were not normally distributed, and Mann-Whitney tests were used.

the mice. Plasma levels of the inflammation marker TNF-α were 44% lower in FURIN inhibitor–treated mice (FURIN inhibitor: 21.6±3.1, n=15; Control: 38.8±7.5 pg/mL, n=14; *P*=0.05; Figure 4A). Similarly, plasma levels of the inflammation marker IL1-β were also significantly lower (by 66%) in the FURIN inhibitor–treated group (FURIN inhibitor: 13.9±2.8, n=15; Control: 40.8±8.9 pg/mL, n=14; *P*=0.01; Figure 4B). Furthermore, we assessed levels of active TGF-β1, an inflammatory cytokine that plays a critical role in extracellular matrix degradation, which is also a substrate for FURIN.[43] Active TGF-β1 levels were significantly lower in the FURIN inhibitor–treated mice (FURIN inhibitor: 45.8±5.1, n=16; Control: 62.0±4.6 pg/mL, n=15; *P*=0.02; Figure 4C), in line with our finding of lower lesional collagen in FURIN inhibitor–treated mice.

## FURIN Inhibitor Treatment Results in Elevated Plasma HDL-Cholesterol Levels

Low levels of plasma apoB-containing lipoproteins are associated with atheroprotection, both in humans and in mice.[44] To determine if lipid levels were altered in the FURIN inhibitor–treated hyperlipidemic *Ldlr*$^{-/-}$ mice, we quantified plasma lipids. Plasma LDLc (FURIN inhibitor: 28.4±1.9; Control:

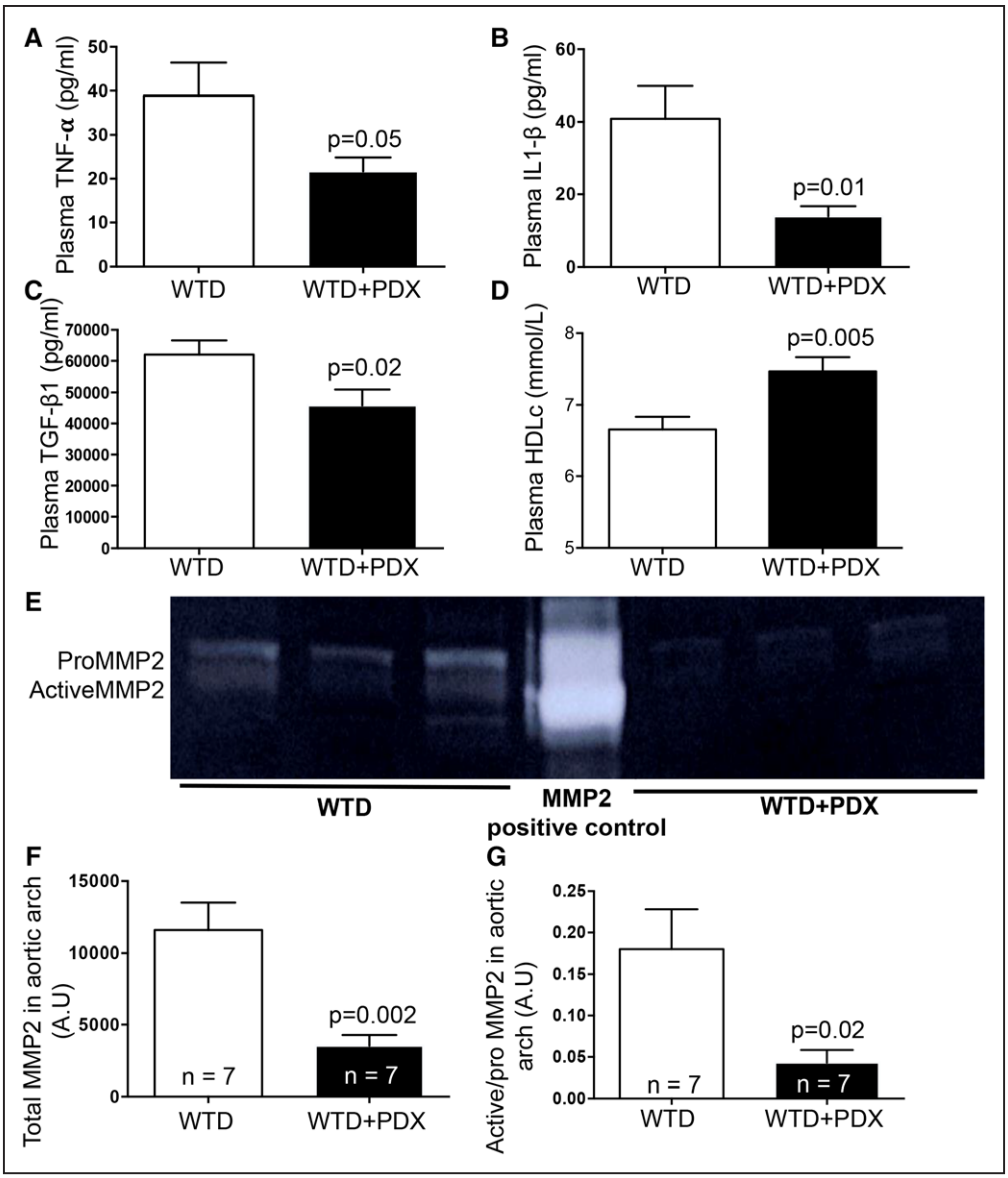


**Figure 4.** Lower plasma inflammatory markers, elevated plasma HDLc (high-density lipoprotein cholesterol), and lower MMP2 (matrix metallopeptidase 2) expression in aorta of FURIN inhibitor–treated mice. Lower plasma levels of (**A**) TNF (tumor necrosis factor)-α, (**B**) IL1 (interleukin 1)-β, (**C**) TGF (transforming growth factor)-β1, and (**D**) elevated plasma HDLc levels in FURIN inhibitor–treated mice. n=14–16 for all analyses. **E**, Gelatin zymography in the aortic arch showing both the pro and active forms of MMP2. **F**, Total MMP2 expression levels are significantly lower in the aortic arch of FURIN inhibitor–treated mice. **G**, Significantly lower active MMP2/proMMP2 expression in the aortic arch of FURIN inhibitor–treated mice. Groups are abbreviated as *Ldlr*$^{-/-}$ mice fed Western-type diet injected with PBS (WTD); *Ldlr*$^{-/-}$ mice fed WTD injected with the α-1-PDX (α1-antitrypsin Portland) FURIN inhibitor (WTD+PDX). Values represent mean±SEM. All mice are male. Data in **A**–**F** are normally distributed, and *P* values were assessed using Student *t* tests. Data in **G** are not normally distributed, and Mann-Whitney test was performed. A.U indicates arbitrary units.



24.6±1.9 mmol/L, n=16 each; *P*=0.1) and triglycerides (FURIN inhibitor: 7.6±0.5; Control: 7.7±0.7 mmol/L, n=16 each; *P*=0.9) did not differ significantly between the groups (Figure IVA and IVB in the online-only Data Supplement). However, HDLc levels were significantly elevated in the FURIN inhibitor–treated mice (FURIN inhibitor: 7.4±0.2; Control: 6.6±0.1 mmol/L, n=16 each; *P*=0.005; Figure 4D).

## FURIN Inhibition Reduces Matrix Metallopeptidase Activation

As a proprotein convertase, FURIN promotes the conversion of Pro-MMP2 to MMP2 via MT-1 MMP (membrane type 1 matrix metallopeptidase) activation.[45] In addition, the absence of MMP2 results in significant decreases in atherosclerotic lesions in *Mmp2*$^{-/-}$×*Apoe*$^{-/-}$ mice.[46] Thus, we hypothesized that the inhibition of FURIN may have reduced atherosclerotic lesion progression in part via the inhibition of MMP2 activity. Indeed, as assessed by gelatin zymography,[47] levels of total MMP2 (FURIN inhibitor: 3530±749; Control: 11580±1919 densitometry arbitrary units, n=7 each; *P*=0.002; Figure 4E and 4F) and active/pro-MMP2 (FURIN inhibitor: 0.043±0.01; Control: 0.18±0.04 arbitrary units, n=7 each; *P*=0.01; Figure 4E and 4G) were significantly decreased in the aortic arch of FURIN inhibitor–treated mice. Although not shown to

be a substrate for FURIN cleavage, MMP9 plays a role in atherosclerosis development,[48] and deficiency of MMP9 reduced atherosclerotic lesions in mice.[49] We observed no changes in MMP9 levels in the aortic arch of FURIN inhibitor–treated mice (FURIN inhibitor: 7359±1435; Control: 5482±542 arbitrary units, n=7 each; *P*=0.24; Figure V in the online-only Data Supplement), suggesting that FURIN inhibition reduced atherosclerotic lesions in part via the modulation of MMP2 but not MMP9 activity.

### Lower Intima Thickening and Plaque Area in FURIN Inhibitor–Treated *Apoe*$^{-/-}$ Mice

Because our in silico genetic association and gene expression analyses implicated FURIN as a possible mediator of vascular remodeling in atherosclerosis, and MMP2 plays an important role in subendothelial basement membrane formation,[50] we next assessed the impact of FURIN inhibition in a wire injury model of vascular remodeling and restenosis. We administered α-1-PDX FURIN inhibitor via transplanted osmotic minipumps to WTD fed *Apoe*$^{-/-}$ mice in which the endothelium of the common carotid artery was injured with a flexible wire, an established model for the study of vascular remodeling in atherosclerosis.[51] Intimal lesions at the denuded regions were assessed in control and FURIN inhibitor–treated mice. Significantly lower (by 54%) intimal thickness (FURIN inhibitor: 34.1±7.2; Control: 73.9±7.4×10$^3$ μm$^2$, n=6; *P*=0.003) as well as total plaque area (by 35%; FURIN inhibitor: 85.7±11.0; Control: 131.5±15.9×10$^3$ μm$^2$, n=6; *P*=0.04) were observed in the FURIN inhibitor–treated mice (Figure 5A–5D), suggesting that inhibition of FURIN resulted in significant protection from vascular restenosis and lesion formation in this mouse model.

### Lower Plaque Cellularity, Macrophage Number and Inflammation in FURIN Inhibitor–Treated Mice

To determine if, in addition to the reduced lesion area, FURIN inhibition also resulted in reduced lesional macrophage number and inflammation, we assessed these parameters in the *Apoe*$^{-/-}$ wire injury model in vivo. Levels of the inflammatory marker TNF-α in the plaque were significantly lower (FURIN inhibitor: 17.5±2.0; Control: 25.8±2.4 arbitrary units/μm$^2$, n=6 each; *P*=0.02; Figure 5E) suggesting that FURIN inhibition reduces plaque inflammation. Levels of the endothelial adhesion molecule ICAM-1 (intercellular adhesion molecule 1) were not changed in FURIN inhibitor–treated mice (Figure 5F). Total cell number (FURIN inhibitor: 178.6±25.6; Control: 438.2±45.0 cells/plaque, n=6 each; *P*<0.0001; Figure 6A), smooth muscle cell number (FURIN inhibitor: 22.4±3.7; Control: 54.2±6.3 cells/plaque, n=6 each; *P*=0.0001; Figure 6B), and macrophage (MAC-2$^+$) number (FURIN inhibitor: 74.9±13.5; Control: 127.5±16.8 cells/plaque, n=6 each; *P*=0.02; Figure 6C) were significantly lower in atherosclerotic lesions of FURIN inhibitor–treated mice. No significant differences in plaque endothelial cell numbers (CD31$^+$) were observed (Figure 6D). Negative control isotype-specific immunoglobulin staining for these antibodies are shown in Figure VI in the online-only Data Supplement. These data show that FURIN inhibition in vivo reduces plaque cellularity, macrophage numbers, and plaque inflammation.

### Increased FURIN Expression Increases Plaque Area in *Apoe*$^{-/-}$ Mice

Our experiments thus far utilized a FURIN inhibitor, α-1-PDX, to determine the impact of reducing FURIN levels on atherosclerotic lesion development in vivo. However, although this inhibitor shows significant efficacy in inhibiting FURIN, it is not entirely selective against FURIN.[19,20] To more directly confirm the role of FURIN in atherosclerotic lesion development, we next administered purified FURIN protein into WTD fed *Apoe*$^{-/-}$ mice harboring a wire injury of the common carotid artery as described above. Significantly higher intimal thickness (FURIN: 126.50±8.91; Control: 75.59±11.05×10$^3$ μm$^2$, n=5–6; *P*=0.005) as well as total lesion area (FURIN: 172.63±7.82; Control: 117.57±12.45×10$^3$ μm$^2$, n=5–6; *P*=0.004) were observed in the lesions at the denuded regions of the carotid in the FURIN overexpressing mice (Figure 7A–7C), confirming that FURIN levels are directly associated with vascular remodeling and lesion development. In addition to intimal lesion area and thickness, we also assessed macrophage and smooth muscle content in the lesions of these mice. A significant increase in lesional smooth muscle area was observed (FURIN: 51.01±5.33; Control: 32.58±4.66×10$^3$ μm$^2$, n=18–19; *P*=0.01; Figure 7D). However, no changes in lesional macrophage (MAC-2$^+$) area (FURIN: 23.40±2.50; Control: 24.69±3.80×10$^3$ μm$^2$, n=18–19; *P*=0.77; Figure 7E) were observed.

## Discussion

We show here that levels of the proprotein convertase FURIN are directly associated with atherosclerosis and restenosis, both in the hyperlipidemic *Ldlr*$^{-/-}$ model of atherosclerosis and in a carotid wire injury model of vascular endothelial remodeling. We find that systemic inhibition of FURIN prevented atherosclerosis progression in mice, in part, through the modulation of MMP2 activity.

In our *Ldlr*$^{-/-}$ mice, a significant reduction in severe lesions with no changes in early lesions was observed after FURIN inhibition, suggesting that FURIN might play a role in the later stages of lesion development. This is in line with the finding that *FURIN* was the most dysregulated primary PCSK in advanced atherosclerotic plaques, with a median RNA overexpression of ≈40-fold compared with nonatherosclerotic control samples.[38] As well, later stage, rupture-prone atherosclerotic lesions contain activated MMPs, including MMP2,[52] that weaken the plaque cap via extracellular matrix degradation.[52,53] MMP2 is a FURIN substrate and is activated by FURIN.[45] Thus, the prevention of vascular MMP2 activation via FURIN inhibition may attenuate the development of severe lesions.

It is possible that reduced MMP2 levels are not the sole mechanism underlying the atheroprotective phenotypes we observe in the face of FURIN inhibition because FURIN has many protein substrates. However, *Mmp2*$^{-/-}$ mice, when crossed to the *Apoe*$^{-/-}$ mice, show a significant reduction in atherosclerotic lesions at the aortic sinus, as

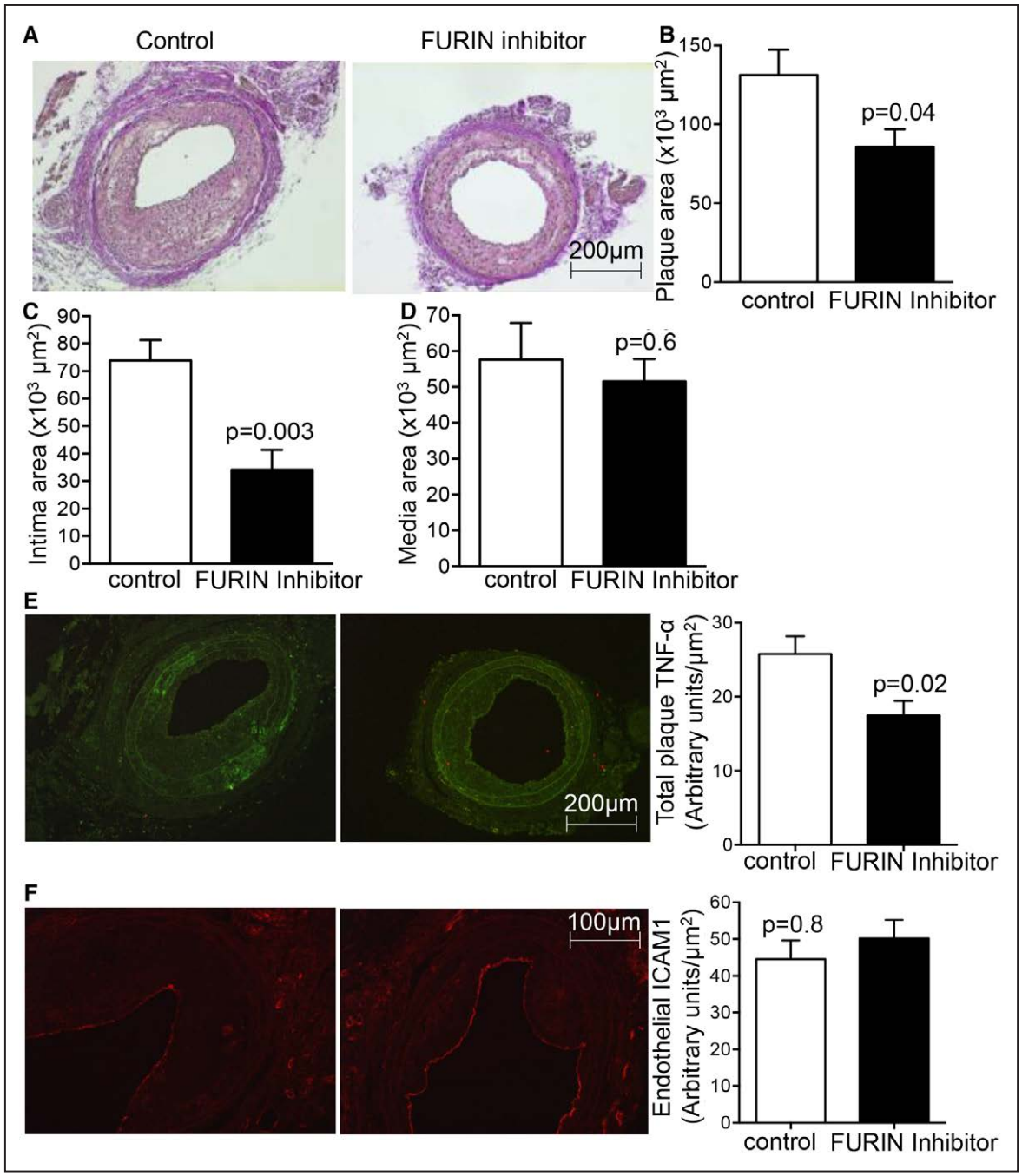


**Figure 5.** FURIN inhibition reduces neointimal plaque formation and inflammation in a wire injury model of atherosclerosis. Male *Apoe*$^{-/-}$ mice were fed a high-fat diet, treated with vehicle (dimethyl sulfoxide [DMSO]) or FURIN Inhibitor α-1-PDX and were subjected to wire injury of the common carotid artery. **A**, Representative photomicrographs of Pentachrome-stained sections 2 wk after injury, (**B**) significantly lower plaque area, (**C**) significantly lower neointima area, and (**D**) unchanged media area in FURIN inhibitor–treated mice. **E**, Significantly decreased vascular inflammatory cytokine TNF (tumor necrosis factor)-α levels (stained in green) and (**F**) unchanged endothelial adhesion molecule ICAM-1 (intercellular adhesion molecule 1) levels (stained in red) in FURIN inhibitor–treated mice. Groups are abbreviated as *Apoe*$^{-/-}$ mice (Control); Apoe$^{-/-}$ mice administered the FURIN inhibitor α-1-PDX (FURIN inhibitor). n=6 per group. Values represent mean±SEM. Data in **A**–**E** are normally distributed, and *P* values were assessed using Student *t* tests. Data in **F** was not normally distributed, and Mann-Whitney test was used.

well as significantly reduced macrophage and collagen content in aortic sinus lesions,[46] similar to our findings in the FURIN inhibitor–treated mice. In addition, no changes were observed in MMP9 levels in the *Mmp2*$^{-/-}$×*Apoe*$^{-/-}$ mice,[46] similar to our findings that MMP9 levels are unaltered in the aortic arch of the FURIN inhibitor–treated mice. The reduced systemic inflammatory markers observed in the face of FURIN inhibition in our mice could also be modulated via the inhibition of MMP2 activity because the chemokine ligands CCL7 (C-C motif chemokine ligand 7) and CXCL-12 (C-X-C motif chemokine ligand 12) are substrates for MMP2[54,55] and *Mmp2*$^{-/-}$ mice display reduced allergic inflammation[56] suggesting a direct role for MMP2 in modulating inflammation.

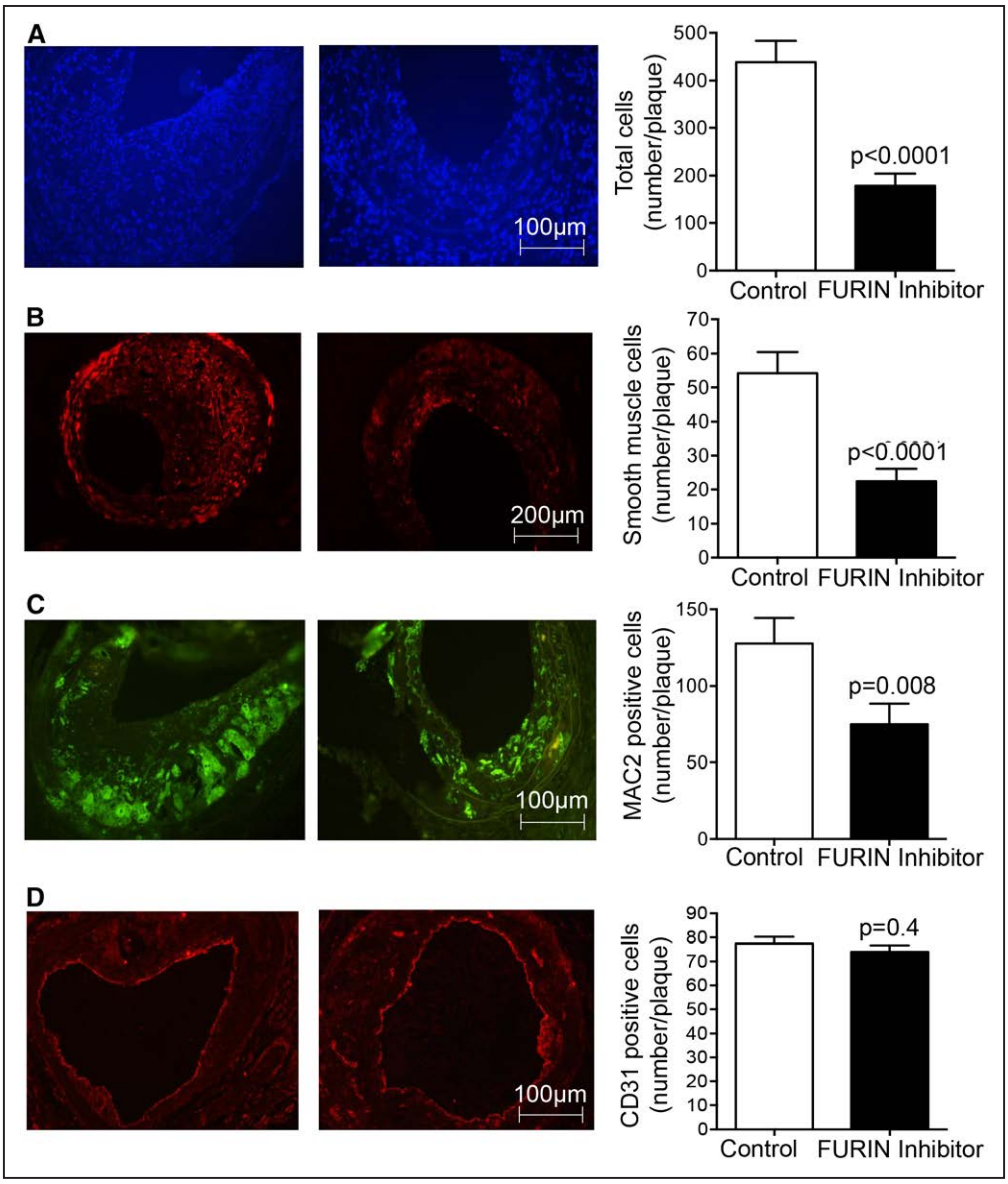


**Figure 6.** FURIN inhibition reduces plaque complexity in a wire injury model of atherosclerosis. Male *Apoe*$^{-/-}$ mice were fed a high-fat diet, treated with vehicle (Control) or FURIN Inhibitor α-1-PDX and subjected to wire-induced injury of the common carotid artery. **A**, The total number of cells, (**B**) the number of smooth muscle cells, and (**C**) the number of MAC-2 (Galectin-3)–positive macrophages per plaque were all significantly lower in FURIN inhibitor–treated mice. **D**, No changes in CD31$^{+}$ endothelial cell numbers were observed. Groups are abbreviated as *Apoe*$^{-/-}$ mice (Control); *Apoe*$^{-/-}$ mice administered the FURIN inhibitor α-1-PDX (FURIN inhibitor). n=6 per group. Values represent mean±SEM. Data in **A**–**C** are not normally distributed, and *P* values were assessed using Mann-Whitney tests. Data in **D** is normally distributed, and Student *t* test was used.

The curated FURIN substrate database, FurinDB (http://www.nuolan.net), lists 87 mammalian substrates for FURIN.[57] These include many proteins with functions in the extracellular matrix, suggesting that one mechanism by which FURIN inhibition may reduce atherosclerotic lesions is via the regulation of the extracellular matrix, which plays a central role in tissue remodeling, as well as cell migration, cytokine, and chemokine recruitment, and adhesion receptor and cell surface proteoglycan recruitment at sites of lesions.[33] In line with a central role for FURIN in tissue remodeling, our data show that FURIN inhibition had a significant impact in reducing lesions in our model of vascular endothelial injury induced atherosclerosis.

Of interest, FURIN is a protease for PCSK9,[58] a critical regulator of LDLc metabolism, with an established role in atherosclerosis.[59] The accepted mechanism at present for PCSK9's role in LDLc metabolism and atherosclerosis is directly related to its role in the LDLR (LDL receptor) pathway. PCSK9 binds to LDLRs at the plasma membrane and targets them to lysosomes for degradation.[60] Since PCSK9 is a substrate for FURIN, to exclude a contribution by PCSK9 in our analyses of atherosclerosis, we chose the *Ldlr*$^{-/-}$ mouse model for part of our experiments. In addition, we saw no changes in plasma LDLc levels in our experiments. However, more recent studies on PCSK9 suggest that it may act in a paracrine manner in the arterial wall.[61] Thus, if PCSK9 might modulate

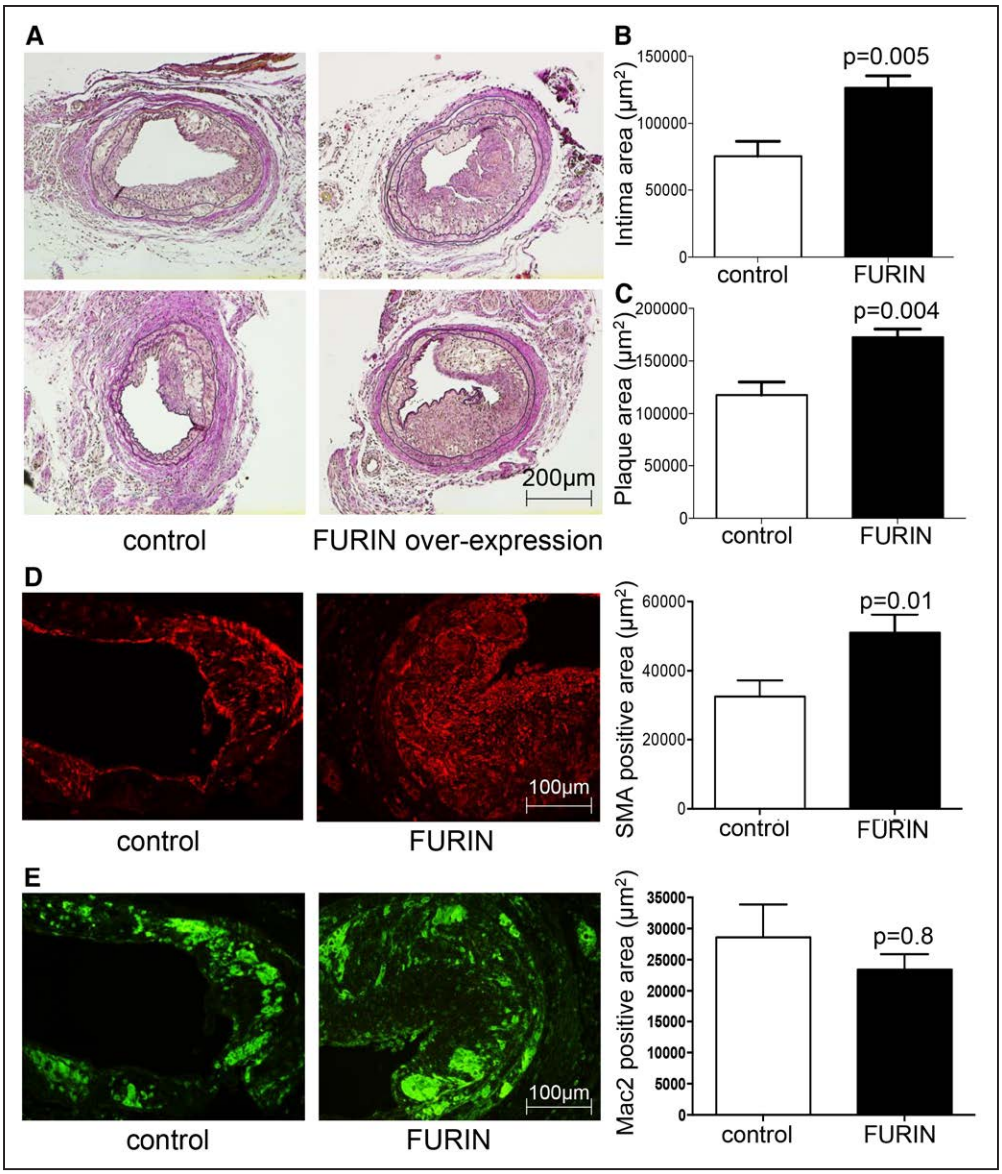


**Figure 7.** FURIN overexpression increases neointimal plaque formation in a wire injury model of atherosclerosis. Male *Apoe*$^{-/-}$ mice were fed a Western-type diet, subjected to wire-induced injury of the common carotid artery, and treated with vehicle (n=5) or purified FURIN protein (n=6). **A**, Representative photomicrographs of Pentachrome-stained sections at 2 wk after injury, and (**B**) significantly higher neointima, and (**C**) plaque area in FURIN protein injected mice. **D**, Significantly increased smooth muscle cell area (stained in red) and (**E**) no change in macrophage area (stained in green) in the lesions of FURIN overexpressing mice. Groups are abbreviated as *Apoe*$^{-/-}$ mice (Control); *Apoe*$^{-/-}$ mice administered purified FURIN protein (FURIN). Values represent mean±SEM. Data in **A**–**D** are normally distributed, and *P* values were assessed using Student *t* tests. Data in **E** is not normally distributed, and the Mann-Whitney test was used. Mac2 indicates Galectin-3; and SMA, smooth muscle actin.

atherosclerosis through LDLR independent mechanisms, and if FURIN might play a role in these mechanisms is unclear.

One potential caveat to our study was considered, which is the substrate specificity of the FURIN inhibitor, α-1-PDX. The α-1-PDX inhibitor was generated by mutating the reactive-site loop of α-1-antitrypsin to contain the minimal consensus sequence for FURIN cleavage,[62] resulting in the generation of an SDS-resistant complex with FURIN through its catalytic serine.[62] α-1-PDX displayed high selectivity for FURIN with Ki values as low as 600 pM[41]. However, at higher concentrations, α-1-PDX can also inhibit PC5/6[41]. If PC5/6 plays a role in atherosclerosis is unknown. As PC5/6 is expressed predominantly in the small intestine, kidney and lung of adult mice,[63] a direct effect of PC5/6 in atherosclerosis is unlikely. Despite the partial nonspecificity of α-1-PDX, in biochemical, cellular and animal studies, α-1-PDX is well established to block FURIN activity.[64] To exclude the possibility that other proteins inhibited by α-1-PDX may have caused the observed reduction in atherosclerotic lesions in our experiments, and to directly confirm that FURIN alone can modulate atherosclerotic processes, we delivered FURIN protein to mice with a vascular endothelial injury in their carotid arteries and found a 67% increase in intimal lesion area in the face of FURIN overexpression, directly implicating a role for FURIN in lesion formation. Of note, the *Arteriosclerosis, Thrombosis, and Vascular Biology* Council recommends the use of both sexes in studies of atherosclerosis.[65] Only male mice were utilized here, which is a limitation of our study.

Our findings suggest that FURIN inhibition may be beneficial for the inhibition of atherosclerosis and restenosis. The prevention of vascular MMP2 activation via FURIN inhibition may constitute an attractive mechanism to attenuate the development of severe lesions and may lead to increased plaque stability, thus representing a new therapeutic option for the treatment of atherosclerosis. Since advanced lesions leading to plaque rupture is the primary driver for CAD-related mortality, this possibility may have far-reaching clinical consequences. Furthermore, due to FURIN's role as an upstream activator of multiple substrates, inhibiting FURIN is likely to provide a broader benefit in lesion development, compared with targeting individual downstream effectors.

## Acknowledgments

We thank Wim van Duyvenvoorde and Marijke Voskuilen for excellent technical assistance in atherosclerotic lesion analyses and Roya Soltan, Melanie Garbe and Nadine Persigehl for their excellent technical assistance in tissue sample preparation and immunohistochemical staining. We certify that all persons who have made substantial contributions to the article but who do not fulfill authorship criteria are named with their specific contributions in the Acknowledgments section of the article and that all persons named in the Acknowledgments section have provided the corresponding author with written permission to be named in the article.

## Sources of Funding

The work in this article was funded by the Singapore Ministry of Education Tier 2 grant (MOE2016-T2-1–122) to S. Ghosh and R.R. Singaraja, as well as by the Agency for Science, Technology and Research and the National University of Singapore to R.R. Singaraja. H.A. Cabrera-Fuentes was supported by the Russian Government Program for competitive growth of Kazan Federal University, Kazan (Russian Federation), by the Singapore Heart Foundation (SHF/FG657P/2017), and by the von Behring-Röntgen-Foundation (Marburg, Germany). D.J. Hausenloy is supported by the Duke-National University Singapore Medical School; Singapore Ministry of Health's National Medical Research Council (NMRC/CSA-SI/0011/2017) and Collaborative Centre Grant (NMRC/CGAug16C006); the Singapore Ministry of Education Tier 2 (MOE2016-T2-2–021); National Institute for Health Research University College London Hospitals Biomedical Research Centre; and the British Heart Foundation (FS/10/039/28270). E.A. Liehn was funded by the Interdisciplinary Center for Clinical Research IZKF (Zentrum für Klinische Forschung) Aachen (Junior Research Group E.A. Liehn). S. Ghosh is supported by the American Heart Association (AHA10SDG4230068), the National Medical Research Council, Singapore, and the Ministry of Health, Singapore.

## Disclosures

None.

## References

1. Barquera S, Pedroza-Tobías A, Medina C, Hernández-Barrera L, Bibbins-Domingo K, Lozano R, Moran AE. Global overview of the epidemiology of atherosclerotic cardiovascular disease. *Arch Med Res*. 2015;46:328–338. doi: 10.1016/j.arcmed.2015.06.006
2. Cannon CP, Braunwald E, McCabe CH, Rader DJ, Rouleau JL, Belder R, Joyal SV, Hill KA, Pfeffer MA, Skene AM; Pravastatin or Atorvastatin Evaluation and Infection Therapy-Thrombolysis in Myocardial Infarction 22 Investigators. Intensive versus moderate lipid lowering with statins after acute coronary syndromes. *N Engl J Med*. 2004;350:1495–1504. doi: 10.1056/NEJMoa040583
3. Preuss M, König IR, Thompson JR, et al; CARDIoGRAM Consortium. Design of the Coronary ARtery DIsease Genome-Wide Replication And Meta-Analysis (CARDIoGRAM) Study: a genome-wide association meta-analysis involving more than 22 000 cases and 60 000 controls. *Circ Cardiovasc Genet*. 2010;3:475–483. doi: 10.1161/CIRCGENETICS.109.899443
4. Ghosh S, Vivar J, Nelson CP, et al. Systems genetics analysis of genome-wide association study reveals novel associations between key biological processes and coronary artery disease. *Arterioscler Thromb Vasc Biol*. 2015;35:1712–1722. doi: 10.1161/ATVBAHA.115.305513
5. Roebroek AJ, Umans L, Pauli IG, Robertson EJ, van Leuven F, Van de Ven WJ, Constam DB. Failure of ventral closure and axial rotation in embryos lacking the proprotein convertase Furin. *Development*. 1998;125:4863–4876.
6. Scamuffa N, Sfaxi F, Ma J, Lalou C, Seidah N, Calvo F, Khatib AM. Prodomain of the proprotein convertase subtilisin/kexin Furin (ppFurin) protects from tumor progression and metastasis. *Carcinogenesis*. 2014;35:528–536. doi: 10.1093/carcin/bgt345
7. Bassi DE, Zhang J, Cenna J, Litwin S, Cukierman E, Klein-Szanto AJ. Proprotein convertase inhibition results in decreased skin cell proliferation, tumorigenesis, and metastasis. *Neoplasia*. 2010;12:516–526.
8. Lin H, Ah Kioon MD, Lalou C, Larghero J, Launay JM, Khatib AM, Cohen-Solal M. Protective role of systemic furin in immune response-induced arthritis. *Arthritis Rheum*. 2012;64:2878–2886. doi: 10.1002/art.34523
9. Wylie JD, Ho JC, Singh S, McCulloch DR, Apte SS. Adamts5 (aggrecanase-2) is widely expressed in the mouse musculoskeletal system and is induced in specific regions of knee joint explants by inflammatory cytokines. *J Orthop Res*. 2012;30:226–233. doi: 10.1002/jor.21508
10. Komiyama T, Swanson JA, Fuller RS. Protection from anthrax toxin-mediated killing of macrophages by the combined effects of furin inhibitors and chloroquine. *Antimicrob Agents Chemother*. 2005;49:3875–3882. doi: 10.1128/AAC.49.9.3875-3882.2005
11. Ozden S, Lucas-Hourani M, Ceccaldi PE, et al. Inhibition of Chikungunya virus infection in cultured human muscle cells by furin inhibitors: impairment of the maturation of the E2 surface glycoprotein. *J Biol Chem*. 2008;283:21899–21908. doi: 10.1074/jbc.M802444200
12. Stawowy P, Kallisch H, Borges Pereira Stawowy N, Stibenz D, Veinot JP, Gräfe M, Seidah NG, Chrétien M, Fleck E, Graf K. Immunohistochemical localization of subtilisin/kexin-like proprotein convertases in human atherosclerosis. *Virchows Arch*. 2005;446:351–359. doi: 10.1007/s00428-004-1198-7
13. Stawowy P, Fleck E. Proprotein convertases furin and PC5: targeting atherosclerosis and restenosis at multiple levels. *J Mol Med (Berl)*. 2005;83:865–875. doi: 10.1007/s00109-005-0723-8
14. Lei X, Basu D, Li Z, Zhang M, Rudic RD, Jiang XC, Jin W. Hepatic overexpression of the prodomain of furin lessens progression of atherosclerosis and reduces vascular remodeling in response to injury. *Atherosclerosis*. 2014;236:121–130. doi: 10.1016/j.atherosclerosis.2014.06.015
15. Fathy SA, Abdel Hamid FF, Zabut BM, Jamee AF, Ali MA, Abu Mustafa AM. Diagnostic utility of BNP, corin and furin as biomarkers for cardiovascular complications in type 2 diabetes mellitus patients. *Biomarkers*. 2015;20:460–469. doi: 10.3109/1354750X.2015.1093032
16. Deloukas P, Kanoni S, Willenborg C, et al; CARDIoGRAMplusC4D Consortium. Large-scale association analysis identifies new risk loci for coronary artery disease. *Nat Genet*. 2013;45:25–33. doi: 10.1038/ng.2480
17. Shiryaev SA, Remacle AG, Ratnikov BI, et al. Targeting host cell furin proprotein convertases as a therapeutic strategy against bacterial toxins and viral pathogens. *J Biol Chem*. 2007;282:20847–20853. doi: 10.1074/jbc.M703847200
18. Ma YC, Fan WJ, Rao SM, Gao L, Bei ZY, Xu ST. Effect of Furin inhibitor on lung adenocarcinoma cell growth and metastasis. *Cancer Cell Int*. 2014;14:43. doi: 10.1186/1475-2867-14-43
19. Seidah NG, Prat A. The biology and therapeutic targeting of the proprotein convertases. *Nat Rev Drug Discov*. 2012;11:367–383.
20. Couture F, Kwiatkowska A, Dory YL, Day R. Therapeutic uses of furin and its inhibitors: a patent review. *Expert Opin Ther Pat*. 2015;25:379–396. doi: 10.1517/13543776.2014.1000303
21. Bassi DE, Lopez De Cicco R, Mahloogi H, Zucker S, Thomas G, Klein-Szanto AJ. Furin inhibition results in absent or decreased invasiveness and tumorigenicity of human cancer cells. *Proc Natl Acad Sci USA*. 2001;98:10326–10331. doi: 10.1073/pnas.191199198
22. Coppola JM, Bhojani MS, Ross BD, Rehemtulla A. A small-molecule furin inhibitor inhibits cancer cell motility and invasiveness. *Neoplasia*. 2008;10:363–370.

23. Mathur R, Rotroff D, Ma J, Shojaie A, Motsinger-Reif A. Gene set analysis methods: a systematic comparison. *BioData Min*. 2018;11:8. doi: 10.1186/s13040-018-0166-8
24. Fabregat A, Jupe S, Matthews L, et al. The reactome pathway knowledgebase. *Nucleic Acids Res*. 2018;46(D1):D649–D655. doi: 10.1093/nar/gkx1132.
25. Daugherty A, Tall AR, Daemen MJAP, Falk E, Fisher EA, García-Cardeña G, Lusis AJ, Owens AP III, Rosenfeld ME, Virmani R; American Heart Association Council on Arteriosclerosis, Thrombosis and Vascular Biology; and Council on Basic Cardiovascular Sciences. Recommendation on design, execution, and reporting of animal atherosclerosis studies: a scientific statement from the American Heart Association. *Arterioscler Thromb Vasc Biol*. 2017;37:e131–e157. doi: 10.1161/ATV.0000000000000062
26. Stary HC, Chandler AB, Dinsmore RE, Fuster V, Glagov S, Insull W Jr, Rosenfeld ME, Schwartz CJ, Wagner WD, Wissler RW. A definition of advanced types of atherosclerotic lesions and a histological classification of atherosclerosis. A report from the Committee on Vascular Lesions of the Council on Arteriosclerosis, American Heart Association. *Arterioscler Thromb Vasc Biol*. 1995;15:1512–1531.
27. Stary HC, Chandler AB, Glagov S, Guyton JR, Insull W Jr, Rosenfeld ME, Schaffer SA, Schwartz CJ, Wagner WD, Wissler RW. A definition of initial, fatty streak, and intermediate lesions of atherosclerosis. A report from the Committee on Vascular Lesions of the Council on Arteriosclerosis, American Heart Association. *Arterioscler Thromb*. 1994;14:840–856.
28. Simsekyilmaz S, Cabrera-Fuentes HA, Meiler S, Kostin S, Baumer Y, Liehn EA, Weber C, Boisvert WA, Preissner KT, Zernecke A. Role of extracellular RNA in atherosclerotic plaque formation in mice. *Circulation*. 2014;129:598–606. doi: 10.1161/CIRCULATIONAHA.113.002562
29. Shagdarsuren E, Bidzhekov K, Djalali-Talab Y, Liehn EA, Hristov M, Matthijsen RA, Buurman WA, Zernecke A, Weber C. C1-esterase inhibitor protects against neointima formation after arterial injury in atherosclerosis-prone mice. *Circulation.* 2008;117:70–78. doi: 10.1161/CIRCULATIONAHA.107.715649
30. Shagdarsuren E, Djalali-Talab Y, Aurrand-Lions M, Bidzhekov K, Liehn EA, Imhof BA, Weber C, Zernecke A. Importance of junctional adhesion molecule-C for neointimal hyperplasia and monocyte recruitment in atherosclerosis-prone mice-brief report. *Arterioscler Thromb Vasc Biol*. 2009;29:1161–1163. doi: 10.1161/ATVBAHA.109.187898
31. Ritz C, Baty F, Streibig JC, Gerhard D. Dose-response analysis using R. *PLoS One*. 2015;10:e0146021. doi: 10.1371/journal.pone.0146021
32. Croft D, Mundo AF, Haw R, et al. The Reactome pathway knowledgebase. *Nucleic Acids Res*. 2014;42(Database issue):D472–D477. doi: 10.1093/nar/gkt1102
33. Katsuda S, Kaji T. Atherosclerosis and extracellular matrix. *J Atheroscler Thromb*. 2003;10:267–274.
34. Hu W, Huang Y. Targeting the platelet-derived growth factor signalling in cardiovascular disease. *Clin Exp Pharmacol Physiol*. 2015;42:1221–1224. doi: 10.1111/1440-1681.12478
35. Rizzo P, Ferrari R. The Notch pathway: a new therapeutic target in atherosclerosis? *Eur Heart J Supp*. 2015;17(A):74–76. doi: 10.1093/eurheartj/ehu244.
36. Toma I, McCaffrey TA. Transforming growth factor-β and atherosclerosis: interwoven atherogenic and atheroprotective aspects. *Cell Tissue Res*. 2012;347:155–175. doi: 10.1007/s00441-011-1189-3
37. Barrett T, Troup DB, Wilhite SE, Ledoux P, Rudnev D, Evangelista C, Kim IF, Soboleva A, Tomashevsky M, Marshall KA, Phillippy KH, Sherman PM, Muertter RN, Edgar R. NCBI GEO: archive for high-throughput functional genomic data. *Nucleic Acids Res*. 2009;37(Database issue):D885–D890. doi: 10.1093/nar/gkn764
38. Turpeinen H, Raitoharju E, Oksanen A, Oksala N, Levula M, Lyytikäinen LP, Järvinen O, Creemers JW, Kähönen M, Laaksonen R, Pelto-Huikko M, Lehtimäki T, Pesu M. Proprotein convertases in human atherosclerotic plaques: the overexpression of FURIN and its substrate cytokines BAFF and APRIL. *Atherosclerosis.* 2011;219:799–806. doi: 10.1016/j.atherosclerosis.2011.08.011
39. Garten W, Hallenberger S, Ortmann D, Schäfer W, Vey M, Angliker H, Shaw E, Klenk HD. Processing of viral glycoproteins by the subtilisin-like endoprotease furin and its inhibition by specific peptidylchloroalkylketones. *Biochimie*. 1994;76:217–225.
40. Kim WJ, Essalmani R, Szumska D, Creemers JWM, Roebroek AJM, D'Orleans-Juste P, Bhattachary S, Seidah NG, Prat A. Loss of endothelial FURIN leads to cardiac malformation and early postnatal death. *Mol Cellular Biol*. 2012:32:3382–3391. doi: 10.1128/MCB.06331-11.
41. Jean F, Stella K, Thomas L, Liu G, Xiang Y, Reason AJ, Thomas G. alpha1-Antitrypsin Portland, a bioengineered serpin highly selective for furin: application as an antipathogenic agent. *Proc Natl Acad Sci USA*. 1998;95:7293–7298.
42. Breslow JL. Mouse models of atherosclerosis. *Science*. 1996;272:685–688.
43. ten Dijke P, Arthur HM. Extracellular control of TGFbeta signalling in vascular development and disease. *Nat Rev Mol Cell Biol*. 2007;8:857–869. doi: 10.1038/nrm2262
44. Shapiro MD, Fazio S. Apolipoprotein B-containing lipoproteins and atherosclerotic cardiovascular disease. *F1000Res*. 2017;6:134. doi: 10.12688/f1000research.9845.1
45. Stawowy P, Meyborg H, Stibenz D, Borges Pereira Stawowy N, Roser M, Thanabalasingam U, Veinot JP, Chrétien M, Seidah NG, Fleck E, Graf K. Furin-like proprotein convertases are central regulators of the membrane type matrix metalloproteinase-pro-matrix metalloproteinase-2 proteolytic cascade in atherosclerosis. *Circulation*. 2005;111:2820–2827. doi: 10.1161/CIRCULATIONAHA.104.502617
46. Kuzuya M, Nakamura K, Sasaki T, Cheng XW, Itohara S, Iguchi A. Effect of MMP-2 deficiency on atherosclerotic lesion formation in apoE-deficient mice. *Arterioscler Thromb Vasc Biol*. 2006;26:1120–1125. doi: 10.1161/01.ATV.0000218496.60097.e0
47. Toth M, Fridman R. Assessment of gelatinases (MMP-2 and MMP-9 by gelatin zymography. *Methods Mol Med*. 2001;57:163–174. doi: 10.1385/1-59259-136-1:163
48. Wågsäter D, Zhu C, Björkegren J, Skogsberg J, Eriksson P. MMP-2 and MMP-9 are prominent matrix metalloproteinases during atherosclerosis development in the Ldlr(−/−)Apob(100/100) mouse. *Int J Mol Med*. 2011;28:247–253. doi: 10.3892/ijmm.2011.693
49. Luttun A, Lutgens E, Manderveld A, Maris K, Collen D, Carmeliet P, Moons L. Loss of matrix metalloproteinase-9 or matrix metalloproteinase-12 protects apolipoprotein E-deficient mice against atherosclerotic media destruction but differentially affects plaque growth. *Circulation*. 2004;109:1408–1414. doi: 10.1161/01.CIR.0000121728.14930.DE
50. Strongin AY, Collier I, Bannikov G, Marmer BL, Grant GA, Goldberg GI. Mechanism of cell surface activation of 72-kDa type IV collagenase. Isolation of the activated form of the membrane metalloprotease. *J Biol Chem*. 1995;270:5331–5338.
51. Lindner V, Fingerle J, Reidy MA. Mouse model of arterial injury. *Circ Res*. 1993;73:792–796.
52. Galis ZS, Sukhova GK, Lark MW, Libby P. Increased expression of matrix metalloproteinases and matrix degrading activity in vulnerable regions of human atherosclerotic plaques. *J Clin Invest*. 1994;94:2493–2503. doi: 10.1172/JCI117619
53. Gough PJ, Gomez IG, Wille PT, Raines EW. Macrophage expression of active MMP-9 induces acute plaque disruption in apoE-deficient mice. *J Clin Invest*. 2006;116:59–69. doi: 10.1172/JCI25074
54. McQuibban GA, Gong JH, Tam EM, McCulloch CA, Clark-Lewis I, Overall CM. Inflammation dampened by gelatinase A cleavage of monocyte chemoattractant protein-3. *Science*. 2000;289:1202–1206.
55. Zhang K, McQuibban GA, Silva C, Butler GS, Johnston JB, Holden J, Clark-Lewis I, Overall CM, Power C. HIV-induced metalloproteinase processing of the chemokine stromal cell derived factor-1 causes neurodegeneration. *Nat Neurosci*. 2003;6:1064–1071. doi: 10.1038/nn1127
56. Corry DB, Rishi K, Kanellis J, Kiss A, Song Lz LZ, Xu J, Feng L, Werb Z, Kheradmand F. Decreased allergic lung inflammatory cell egression and increased susceptibility to asphyxiation in MMP2-deficiency. *Nat Immunol*. 2002;3:347–353. doi: 10.1038/ni773
57. Tian S, Huang Q, Fang Y, Wu J. FurinDB: a database of 20-residue furin cleavage site motifs, substrates and their associated drugs. *Int J Mol Sci*. 2011;12:1060–1065.
58. Benjannet S, Rhainds D, Hamelin J, Nassoury N, Seidah NG. The proprotein convertase (PC) PCSK9 is inactivated by furin and/or PC5/6A: functional consequences of natural mutations and post-translational modifications. *J Biol Chem*. 2006;281:30561–30572. doi: 10.1074/jbc.M606495200
59. Cariou B, Le May C, Costet P. Clinical aspects of PCSK9. *Atherosclerosis*. 2011;216:258–265. doi: 10.1016/j.atherosclerosis.2011.04.018
60. Cariou B, Ding Z, Mehta JL. PCSK9 and atherosclerosis: beyond LDL-cholesterol lowering. *Atherosclerosis*. 2016;253:275–277. doi: 10.1016/j.atherosclerosis.2016.08.007
61. Ferri N, Marchianò S, Tibolla G, Baetta R, Dhyani A, Ruscica M, Uboldi P, Catapano AL, Corsini A. PCSK9 knock-out mice are protected from neointimal formation in response to perivascular carotid collar placement. *Atherosclerosis*. 2016;253:214–224. doi: 10.1016/j.atherosclerosis.2016.07.910

62. Anderson ED, Thomas L, Hayflick JS, Thomas G. Inhibition of HIV-1 gp160-dependent membrane fusion by a furin-directed α1-antitrypsin variant. *J Biol Chem*. 1993;268:24887–24891.
63. Essalmani R, Hamelin J, Marcinkiewicz J, Chamberland A, Mbikay M, Chrétien M, Seidah NG, Prat A. Deletion of the gene encoding proprotein convertase 5/6 causes early embryonic lethality in the mouse. *Mol Cell Biol*. 2006;26:354–361. doi: 10.1128/MCB.26.1.354-361.2006
64. Molloy SS, Thomas G. Furin. In: Dalbey RE, Sigman DS, eds. *The Enzymes*, Vol. XXII, 3rd Ed. San Diego, CA: Academic Press; 2002:199–235.
65. Robinet P, Milewicz DM, Cassis LA, Leeper NJ, Lu HS, Smith JD. Consideration of sex differences in design and reporting of experimental arterial pathology studies-statement from ATVB council. *Arterioscler Thromb Vasc Biol*. 2018;38:292–303. doi: 10.1161/ATVBAHA.117.309524

## Highlights

- Inhibition of FURIN in vitro reduced monocyte transmigration and macrophage and vascular endothelial cell inflammatory gene expression.
- Inhibition of FURIN in a wire-injured *Apoe*$^{-/-}$ model of vascular remodeling resulted in lower lesion area and lower intima thickening.
- Inhibition of FURIN in Western-type diet fed *Ldlr*$^{-/-}$ mice reduced severe atherosclerotic lesions.
- Overexpression of FURIN significantly increased intimal lesions in the wire injury model of atherosclerosis, confirming a direct role for FURIN in atherosclerosis.
- MMP2 (matrix metallopeptidase) activity is significantly lower in aortic arch of FURIN inhibitor–treated mice, suggesting a contribution to lesion reduction.